PHYSICAL REVIEW B VOLUME 36, NUMBER 2 15 JULY 1987-I

Low-energy electron diffraction study of molecular oxygen physisorbed on graphite

Michael F. Toney* and Samuel C. Fain, Jr.
Department of Physics (FM-15), University of Washington, Seattle, Washington 98195
(Received 28 January 1987)

Monolayers of molecular oxygen physically adsorbed on single-crystal graphite have been studied using low-energy electron diffraction (LEED). The lattice parameters for the low-coverage oblique δ phase and the higher-coverage centered-rectangular δ^* phase are presented as a function of density and compared with x-ray studies. New information about the δ' phase (which is oriented differently on the substrate) indicates that it may be an equilibrium phase. Three different phases are observed at temperatures above those where the δ, δ^*, or δ' phases exist: a low-coverage liquid, an intermediate-coverage θ phase, and a high-coverage fluid phase. The liquid and fluid phases have molecular-axis disorder, sufficient short-range order to produce LEED patterns, and bond-orientational order. We discuss the properties of these phases and the nature of the θ phase, which we believe is a two-dimensional solid with molecular-axis disorder. Our data provide a detailed monolayer density-temperature phase diagram.

I. INTRODUCTION

There has been a great deal of work on the structure, thermodynamics, and phase transitions of monolayers of simple atoms and molecules physisorbed on the basal plane of graphite.[1] These adsorbed layers provide a realization of two-dimensional (2D) condensed matter that can be compared with theoretical models and relatively simple calculations. Because the graphite substrate is energetically very smooth, the effect of the lateral modulation of the adsorption energy caused by the substrate periodicity is small. In addition, graphite is available in several forms with large, homogeneous regions of the basal-plane adsorption surface; this enables adsorbed layers to be probed by numerous experimental techniques.[2]

Physisorbed O_2 on graphite produces a particularly rich and diverse phase diagram summarized in Fig. 1. In Fig. 1(a) a schematic 2D spreading-pressure–versus–temperature phase diagram shows all the phases. The two-phase coexistence regions and possible continuous transitions show up as lines on this diagram. Triple points occur at intersections of the lines. Figure 1(b) shows the more complicated density-versus-temperature phase diagram constructed from monolayer densities inferred from low-energy electron diffraction (LEED),[3–6] neutron diffraction,[7,8] and x-ray diffraction studies.[9–11] Note that the critical-temperature[12,13]–to–triple-temperature ratio[14–17] is $66/26=2.5$. This is twice as large as most 2D systems[2] and will be discussed in Sec. IV.

The structure of the low-coverage, low-temperature δ phase has been studied by neutron,[7,8] x-ray diffraction,[9–11] and computer simulation,[18–23] as well as our earlier LEED work.[3,4] Our earlier LEED data[3] were presented as a function of coverage deduced by comparing δ-phase melting temperatures determined by LEED with those determined using heat-capacity[14] measurements on Grafoil. We give LEED data here as a function of the directly measured monolayer density and compare the LEED and x-ray data directly. Some data not available when Ref. 3 was published are also included. In addition, further information is given about conditions under which the δ' phase is observed.

At higher coverages, the ζ_1 and ζ_2 phases occur.[5] To briefly recapitulate, the ζ_1 phase is a monolayer phase,[6] is stable between 12 and 18 K, and has an incommensurate oblique mesh (slightly distorted from a triangle).[5] The ζ_2 phase is also a monolayer phase, is stable between 18 and 38 K, and has an incommensurate simple triangular mesh; there is a transition between these two phases at about 18 K.[5] The ζ_1-ζ_2 transition has been detected in heat-capacity measurements.[24] At these coverages we also observe diffraction from a structure denoted ζ', which has a mesh that is similar to the ζ_2 but has a very different rotational epitaxy.[5] Because the ζ' structure exists at the same densities and temperatures as the ζ_1 and ζ_2 phase, it is not shown on our phase diagrams. We believe the ζ structure is stabilized by defects on our graphite substrates. We were not able to observe with LEED the high-density, antiferromagnetically ordered ϵ phase,[7,8,11] due to slow ordering kinetics.[25]

We present here data on the higher-temperature liquid θ and fluid phases shown in Fig. 1. We find that the liquid and fluid phases are sufficiently well correlated to produce six diffuse diffraction spots. The θ phase was first detected in our measurements;[4] data presented in Sec. IV indicate that the θ phase is probably a solid. We further discuss the nature of these phases including their rotational epitaxy and the bond-orientational order in the liquid and fluid phases. We also discuss the phase transitions and qualitatively compare our data with heat-capacity and magnetic susceptibility data.

As mentioned above, O_2 on graphite has been investigated by several experimental techniques at various laboratories. For example, heat-capacity measurements have been carried out in three laboratories.[14–16] In all investigations there is a wide variation in gas filling of the cells required to produce a given phase transition temper-

ature between 26 and 32 K, suggesting serious problems with alternate-site adsorption, clustering, and/or intergranular condensation when using large-area substrates.[6] Thus, the coverage scales deduced from filling are not reproducible from study to study, and measurements at the same filling and temperature but from two different samples can give two different locations on the phase diagram. For this reason we have redrawn the phase diagram [Fig. 1(b)] to show the phases as a function of monolayer density instead of the coverage indirectly inferred as in Ref. 4. To use information from techniques not directly measuring monolayer density, we assume there is a unique relationship between monolayer density and phase transition temperature.

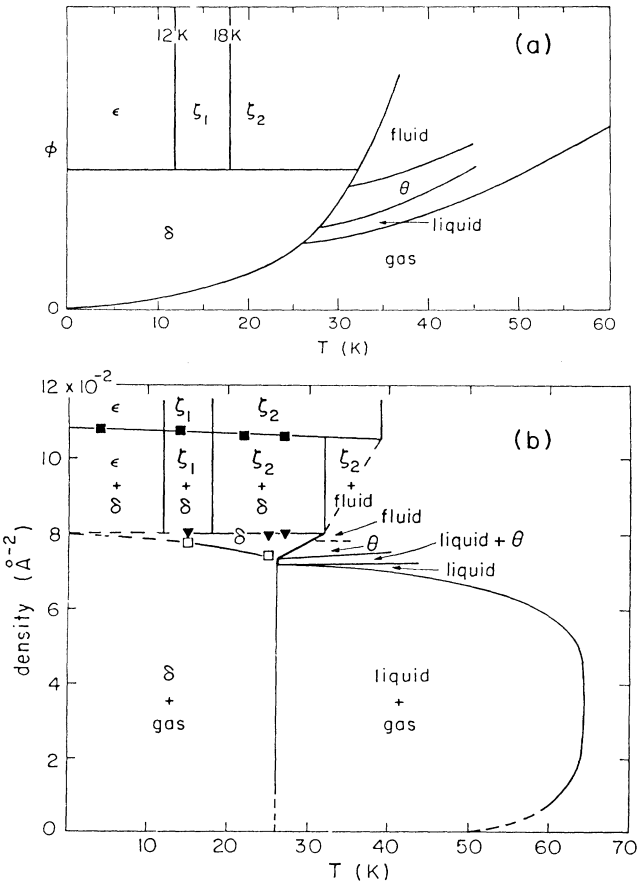

FIG. 1. Tentative phase diagrams of O_2 adsorbed on graphite. (a) Schematic 2D spreading pressure versus temperature diagram. (b) Monolayer density versus temperature diagram. This is a density-temperature phase diagram, rather than a coverage-temperature phase diagram as in Ref. 4; adsorption in the second layer (if any) is not shown. The monolayer densities are deduced from the mesh parameters measured from the diffraction patterns from this study, neutron studies (Refs. 7 and 8), and x-ray studies (Refs. 9–11). The dashed lines are more speculative phase boundaries than the solid lines. Some narrow coexistence regions are not shown. Open squares are the δ-phase densities at the δ-gas phase boundary. Solid inverted triangles are the δ-phase densities at the δ-ζ_2 ($T > 18$ K) or δ-ζ_1 (12 K $< T <$ 18 K) phase boundaries. Solid squares are the ζ_1 or ζ_2 densities at the δ-ζ_1 or δ-ζ_2 phase boundaries.

II. EXPERIMENTAL TECHNIQUES

The experimental apparatus used in this study was essentially the same as that described earlier.[3] Typical base pressures were below 2×10^{-10} Torr as measured by a bare Bayard-Alpert gauge. The residual gases in the system were measured with a quadrupole mass spectrometer and primarily consisted of H_2, CO_2, and $N_2 + CO$, at partial pressures of around 5×10^{-11} Torr; CH_4 and H_2O were also present with partial pressures of about 2×10^{-11} Torr. Experiments were limited in duration to less than 2 h to minimize effects of these residual gases. The LEED electron gun was typically operated at 50–200 eV and about 0.1–1 nA, with a spot diameter of about 0.35 mm full width at half maximum (FWHM).

The graphite samples used in this study were natural single crystals cleaved in air with Scotch tape, baked to between 850 and 980 °C in flowing dry nitrogen gas, and then clamped to the copper sample holder. Baking above 950°C generally produced the best crystals. The graphite substrate was mounted in the vacuum system on a copper sample holder, which was attached to the end of a helium-transfer system. The temperature of the sample holder was measured with a silicon-diode thermometer, which was calibrated against a germanium resistance thermometer. The germanium resistor was factory calibrated between 4 and 75 K. The error in the relative temperatures (temperature differences) is about 0.1 K; the error in absolute temperature is about 1 K.

Occasionally, an impurity LEED pattern was initially observed from the graphite crystals and O_2 would not order on regions of the crystal where this pattern was present. Electron bombardment of the crystal at high current densities (up to 100 nA in 0.1 mm^2) removed the pattern and enabled ordered adsorption.[26] Some crystals initially showed no detectable impurity pattern, and O_2 would order without the electron bombardment treatment. After cooling to very low temperatures (less than about 18 K), there was an irreversible degradation of the crystal which was indicated by an increase in both the size of the overlayer spots and the diffuse background. The degraded crystal had to be replaced or recleaved in order to resolve small spot splittings such as shown here for the θ phase (Fig. 8).

Results from two types of experiments are described here. For experiments at temperatures less than about 32 K, the equilibrium O_2 vapor pressure was very low. A small amount of O_2 gas was admitted through a leak valve and directed at the sample with a doser-doser.[3] Any gas that adsorbed on the surface would not desorb in our experimental times and a continuous flux of gas was not needed to maintain a constant coverage. Coverage was increased by dosing the crystal with additional gas when the temperature was high enough to ensure surface equilibration ($T > 24$ K). The δ phase was always studied under these conditions, and the liquid and θ phases were studied under these conditions if the temperature and coverage were sufficiently low.

At temperatures above about 32 K, some experiments were performed under steady-state adsorption-desorption conditions, with the doser-doser directing a continuous

flux of gas at the sample. Data were taken isothermally as the effective equilibrium pressure at the sample was increased. The impurity gases consisted primarily of N_2 and CO, with a partial pressure of less than 10% of the total vacuum-system pressure. At the sample, the effective $N_2 + CO$ partial pressure was estimated to be less than 1% of the effective total pressure when the doser-doser was in use, due to the higher O_2 partial pressure near the doser-doser.[27] The liquid, θ, and fluid phases were sometimes studied under these conditions.

The LEED patterns from O_2 on graphite were photographed with a 35-mm camera using 400-ASA black and white film. The patterns were analyzed by projecting an image of a LEED pattern onto graph paper. The centers of the diffraction spots were located visually, marked on the graph paper, and digitized. The positions of the diffraction spots were then fit by the least-squares method to the previously determined appropriate unit mesh.

The patterns from the liquid, θ, and fluid phases had six diffuse diffraction spots (not resolution-limited diffraction spots) and were also analyzed by measuring the radial and azimuthal (angular) widths of the diffraction spots using a calibrated microdensitometer.[28] Due to fluctuations in the film density and uncertainties in the background LEED intensity, the widths of the diffraction spots were estimated by visual fits to the intensity obtained from the densitometer. The accuracy of the resulting widths is estimated to be 10%.

III. THE δ PHASE

A. Structures and LEED patterns

The δ phase is the solid phase of O_2 on graphite in which the molecules are inferred to lie essentially parallel to the substrate.[3,9,10] The phase diagram indicates only one δ phase, but three different types of LEED patterns are observed, as shown in Figs. 2(a)–2(c). [Schematic drawings of the patterns in Figs. 2(b) and 2(c) were given in Ref. 3.] At the lowest coverages, the pattern shown in Fig. 2(a) is observed. The circles indicate reflections from one domain of this structure.[3] (One sample once showed a monodomain diffraction pattern which was consistent with that indicated by the circles.) As the coverage is increased by dosing near 24 K, the pattern always changes to that shown in Fig. 2(b).[6] We call the phases producing the pattern in Figs. 2(a) and 2(b) the δ and δ* phases; coexistence between these phases has been observed.[6] At coverages where the δ* phase usually exists, the LEED patterns of Figs. 2(c) and 2(d) are sometimes seen.[3] Although the diffraction pattern in Fig. 2(c) looks very different from that in Fig. 2(b), the structure is the same for Figs. 2(c) and 2(b) except for the azimuthal orientation of the overlayer with respect to the substrate (the rotational epitaxy).[3] In Fig. 2(d) the δ′ phase coexists with the fluid phase to be discussed in Sec. IV.

The structures inferred from the LEED patterns of Fig. 2 are shown in Fig. 3. The 0.002-a.u. electron density contour[4,29] used in Fig. 3 is a more accurate representation of the molecular size than the shape used in Ref. 3. The unit mesh of the δ phase is incommensurate and oblique at low densities, as shown in Fig. 3(a) and first proposed in the x-ray study of Ref. 10. The molecular contours in Fig. 3 have been drawn parallel to the long axis of the parallelogram unit cell shown by dashed lines, as expected from steric considerations.[10,18]

One interesting aspect of the azimuthal orientation of the δ phase shown in Figs. 3(a) and 3(b) and the ζ_2 phase shown in Fig. 2 of Ref. 5 is that rotating the molecules of Fig. 3(b) about the a direction and close packing them together approximately produces the ζ_2 structure shown in Fig. 2 of Ref. 5. This indicates that there may be some common origin of the rotational epitaxy of these structures. (The fact that the molecules stand up in the higher density ζ_1 and ζ_2 phases is a result of the competition between adsorbate-adsorbate and adsorbate-substrate forces.[18])

The unit mesh of the δ phase is incommensurate at all densities, but becomes the centered rectangular δ* phase as the density is increased by dosing near 24 K. The molecular charge contours used for Fig. 3 show that the molecules are close packed in this phase. The angle γ is equal to 90° within experimental error.[3,10,11] Our measurements are not extensive enough to establish the precise region of existence of the δ* and δ′ phases, so we indicate only one δ phase in phase diagrams in Figs. 1 and 9. The δ′ phase will be discussed in more detail below.

B. Lattice parameters versus density

Our lattice-parameter measurements are presented in Fig. 4 as a function of the experimentally calculated monolayer density. This permits us to compare our lattice-parameter measurements near 24 K (solid circles with error bars) with those of x-ray measurements (×'s) on exfoliated graphite substrates at a variety of temperatures and coverages.[10,11] The melting temperatures experimentally observed for the experiments indicated by solid circles are also given in Fig. 4. All the LEED data shown were obtained by dosing the surface below 25 K and then warming up the sample to obtain the melting temperature.

A first-order transition to the centered rectangular δ* phase occurs as the coverage is increased at 24 K. When γ is equal within experimental accuracy to 90°, a rotational-epitaxy angle of $\phi = 3°$ is observed. At lower densities where γ is about 92°, ϕ is always about 0°. This correlation between γ and ϕ also holds for some nonequilibrium measurements not shown in Fig. 4. This correlation suggests that the distortion of the unit cell into the oblique structure observed at low coverages is caused by the rotational epitaxy.

The LEED data in Fig. 4, indicated by solid circles, can be interpreted as indicating a first-order transition between the oblique δ and the centered rectangular δ*. Although the x-ray data shown by ×'s suggest a continuous variation in γ with density, these data were taken at a lower temperature (15 K), and the analysis of these data did not consider the possibility of coexisting phases of different density and γ values.[10] Synchrotron-x-ray measurements on the δ phase at a density of 0.0802 $Å^{-2}$ find a γ between 90° and 90.03° at about 30 K.[11] However,

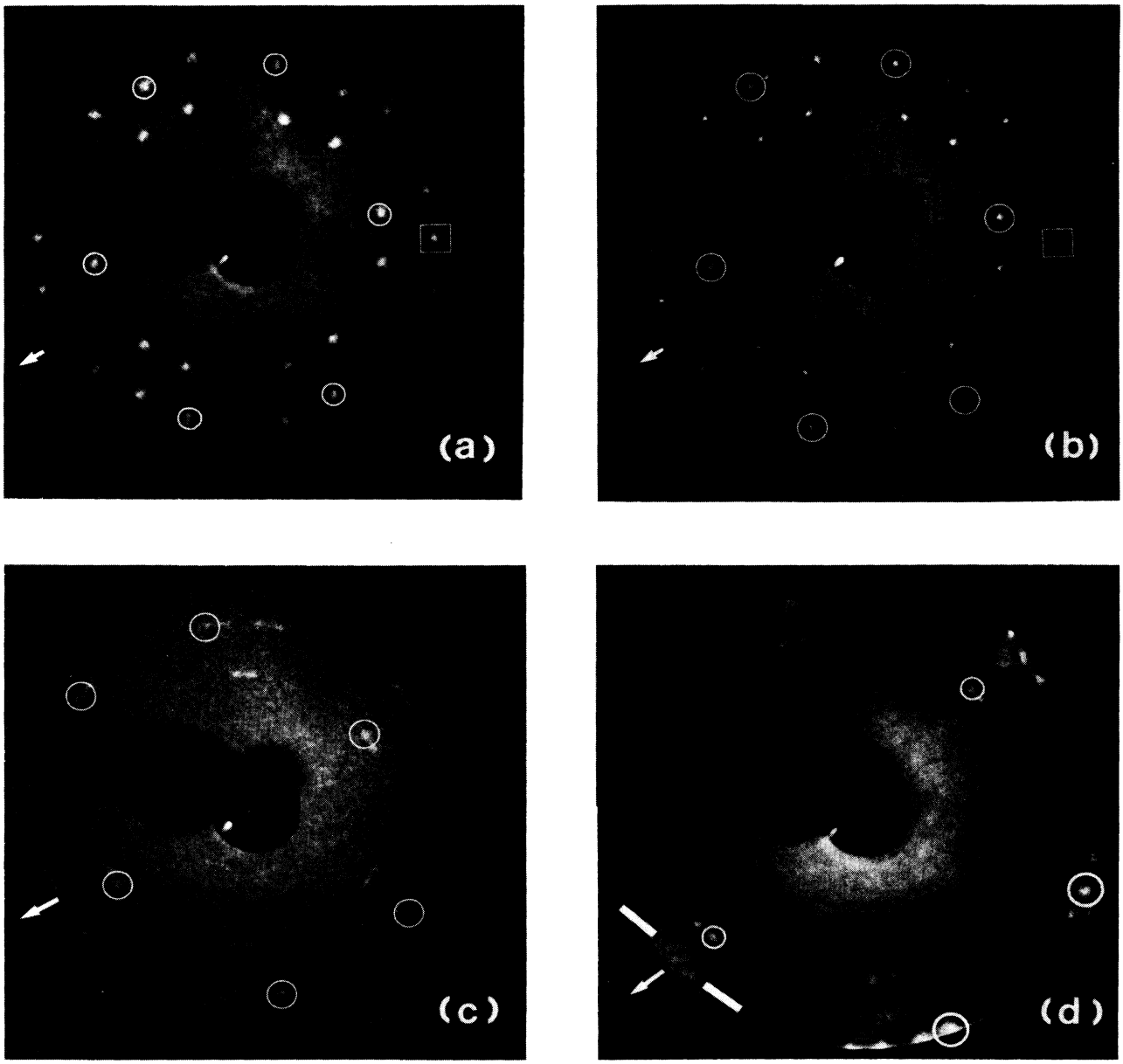

FIG. 2. LEED patterns from the δ phase. The diffraction from one domain is indicated by the circles. The squares indicate one set of spots that is split in (b), but almost degenerate in (a). The arrows indicate the direction of a graphite first-order diffraction vector. There is some distortion caused by the LEED apparatus in the upper right corners of (a) and (d). (a) The low-coverage δ phase at an electron energy of 110 eV, a temperature of 23 K, and a density of 0.075 $Å^{-2}$. (b) The high-coverage δ* phase at 110 eV, 21 K, and 0.077 $Å^{-2}$. (c) The δ′ phase at 112 eV, 16 K, and a density of 0.080 $Å^{-2}$. The azimuthal smearing of the spots is discussed in Ref. 3. (d) The δ′ phase at 65 eV, 31.8 K, and a density at which the δ′ phase coexists with the fluid phase discussed in Sec. IV. One diffraction spot from the fluid phase is located between the two white lines. The different graphite orientation is due to a different graphite substrate than (a)–(c).

these high-resolution measurements did not determine the variation of γ with density and could not determine ϕ.

Zero-temperature calculations for O_2 monolayers on a smooth graphite substrate indicate a centered-rectangular mesh ($\gamma = 90°$) at low coverages,[18,19,22,23] with a and b close to those measured. This confirms our idea that the skewing of the δ-phase mesh into an oblique mesh ($\gamma \neq 90°$) could be caused by the lateral modulation of the adsorption energy by the substrate periodicity. If this lateral variation in energy is included, certain long-period superlattice structures result in a skewing of the unit mesh ($\gamma > 90°$) and an orientational epitaxy angle ϕ close to

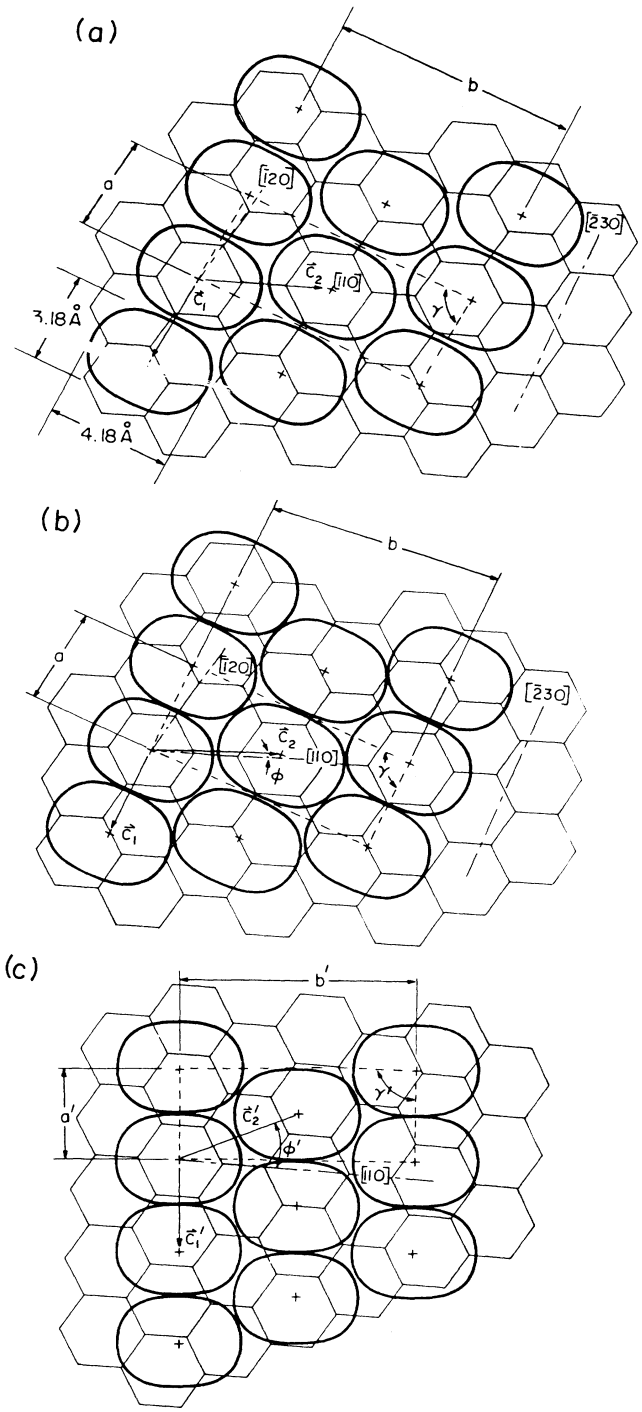

FIG. 3. Structure of one domain of the δ phase on graphite. The oblique unit mesh parameters a, b, and γ, and the primitive mesh vectors $\mathbf{c}_1$ and $\mathbf{c}_2$ are shown. The angle ϕ between the graphite [110] direction and $\mathbf{c}_2$ describes the rotational epitaxy. One molecule is arbitrarily shown in the center of a hexagon. The indicated size of the molecule is the 0.002 electron density contour of Ref. 29. (a) The low-coverage δ-phase structure drawn for a density of 0.074 Å^{-2} and angles $\gamma=92°$ and $\phi=0°$. (b) The high-coverage δ*-phase structure drawn for a density of 0.080 Å^{-2} and angles $\gamma=90°$ and $\phi=3°$. (c) The δ′ phase structure drawn for the density and γ of (b), but angle $\phi'=26°$ as observed in Figs. 2(c) and 2(d).

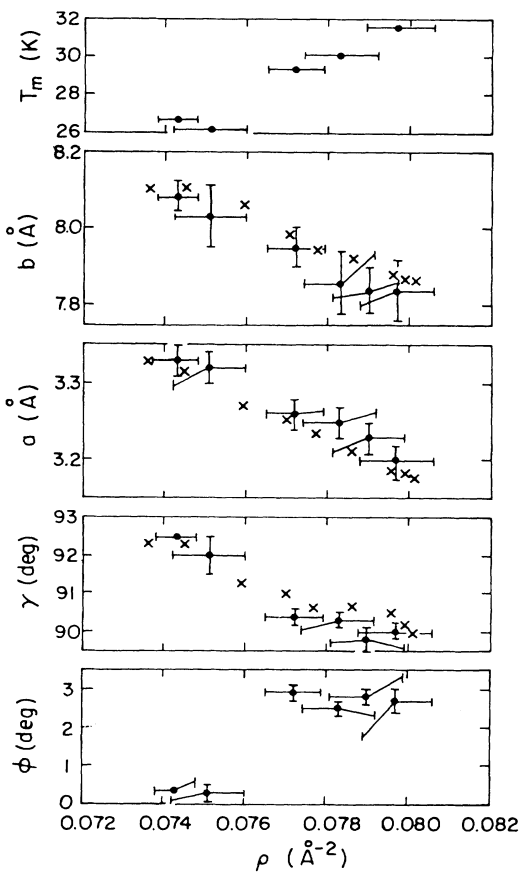

FIG. 4. Mesh parameters of the δ phase as a function of density. The mesh parameters a, b, and γ, and rotational epitaxy angle ϕ are shown for LEED data near 24 K by the solid circles with error bars. X-ray data at various temperatures and coverages are shown as ×'s. The melting temperatures for the LEED measurements are shown in the upper panel.

those found in Fig. 4.[20] One simple long-period commensurate structure was considered in Ref. 3, but the a and γ values of experiment ruled out this structure. The presence of such structures close to the experimentally observed lattice parameters can affect the orientational epitaxy even if the overlayer is incommensurate.[3,30–32]

C. The δ′ phase

The mesh parameters a', b', and γ' for the δ′ phase are the same as a, b, and γ for the densest δ phase; however, the rotational epitaxy of the δ′ phase (described by ϕ') is very different from that of the δ phase. Two structures with reciprocal-lattice vectors of about the same magnitude, but with different rotational epitaxies, are also observed for the higher-coverage ζ phase.[5] The x-ray diffraction studies would probably not have been able to distinguish between the higher-density δ* and δ′ phases, since the mesh constants of the two phases are identical.

The δ′ phase could not be formed by simply adding O_2 to the δ phase (i.e., by dosing the crystal at temperatures

less than 30 K). However, it could be reproducibly formed by cooling the substrate to between about 30 and 34 K and then dosing the sample sufficiently that the layer would solidify when cooled to below 30 K. When the crystal was cooled to below 30 K and then the sample slowly dosed to produce the same solid density, the high-coverage δ^* phase in Fig. 2(b) would always form. When this phase was then warmed to slightly above the melting temperature (30–32 K) and recooled, the δ' phase would form. When this thermal cycling was performed and the dose was insufficient to produce a melting temperature above 30 K, some regions of the crystal had the δ' phase while others had the high coverage δ^*. This last effect could be due to slightly different coverages on the different regions of the crystal. It is possible that the coverage at which the δ' phase could be formed depended on whether the graphite impurity pattern[3,26] was initially present or not, but this has not been carefully examined.

The behavior discussed above suggests that at high coverage the δ' phase may be the equilibrium structure. At these high coverages, the δ^* phase is then metastable, but it cannot transform into the δ' phase because of insufficient surface mobility in the solid.[25] It is possible that at high coverage the Novaco-McTague energy (the overlayer-graphite energy as a function of the alignment of the overlayer) has two local minima at different rotational epitaxies, as discussed in Ref. 3 and predicted for the triangular-incommensurate structure of Xe on graphite.[30,31] At high coverage, the δ' phase may then be in the global minimum and the δ^* may be in a local minimum. At lower coverages there would only be one minimum corresponding to the δ phase. It is also possible that the rotational epitaxy of the δ' phase is stabilized by steps, or impurity adsorption; however, this is less likely since both structures were reproducibly observed on all crystals.

IV. HIGHER TEMPERATURE PHASES: LIQUID, θ, AND FLUID

Three different phases are observed for adsorbed layers of O_2 at temperatures above those where the δ phase exists: a low-coverage liquid phase,[33] an intermediate-coverage θ phase, and a high-coverage fluid phase. Typical LEED patterns from these three phases are shown in Fig. 5. The direction of a graphite first-order reflection (outside the field of view for the energies of Fig. 5) is shown by an arrow in each figure. The liquid [Figs. 5(a) and 5(b)] is characterized by six broad first-order reflections of scattering vector length near 1.80 Å^{-1} and orientation along the direction of the first-order reflections from a $\sqrt{3}$ structure. (A $\sqrt{3}$ structure would have a momentum transfer of 1.70 Å^{-1} and orientation 30° from the arrows in Fig. 5.) The θ phase [Figs. 5(b) and 5(c)] is typically characterized by twelve sharper first-order reflections of scattering vector about 1.84 Å^{-1} and orientation about ±20° from the $\sqrt{3}$ direction (±10° from the arrows in Fig. 5). Diffraction from a single domain of the θ phase is indicated by circles in Figs. 5(b) and 5(c). [An almost monodomain θ phase was observed during the same experiment as Fig. 5(c); normally the two domains had similar intensity.] We believe the θ phase is a solid (see below). The fluid phase [Figs. 5(d) and 2(d)] is characterized by six broad first-order reflections of scattering vector about 1.86 Å^{-1} and orientation 30° from the $\sqrt{3}$ direction (along the arrows in Fig. 5).

The local structure deduced from these patterns is shown in Fig. 6. As there is no indication in the LEED patterns of spots expected from molecular-axis orientational order, the O_2 molecule is represented in these figures as a sphere of the diameter 3.80 Å deduced from studies of 3D liquid O_2.[34] Since the O_2 molecule is about 4.18 Å long, steric considerations suggest the molecules are undergoing hindered rotation with some tilting out of the plane. The liquid [Fig. 6(a)] and fluid [Fig. 6(c)] phases do not have long range positional order; the figure is drawn to show the bond-orientational direction and the approximate average intermolecular spacing. None of these phases has been detected in previous diffraction studies using exfoliated graphite[7–11] due to interference from the graphite (002) diffraction peak (momentum transfer 1.86 Å^{-1}) in polycrystalline samples and to low scattering intensity. (The wings of the liquid diffraction spots were noted in Ref. 10.)

The nearest-neighbor spacing of the liquid and θ phases as a function of temperature is shown in Fig. 7 for coverages near the coexistence boundaries.[35] The circles and triangles indicate the upper and lower nearest-neighbor spacing limits of the liquid phase. These points suggest an increasing density range for the liquid with increasing temperature. The solid squares indicate a slight decrease in nearest-neighbor distance for the θ phase with increasing temperature. This decrease may be related to small changes in the rotational motion of the O_2 molecules, with the molecule behaving more like a free (3D) rotor at higher temperatures.

The azimuthal and radial widths of the diffraction spots for the liquid and θ phases do not appear to change with temperature (between 30 and 48 K) at constant coverage near the liquid-θ phase boundary or near the liquid-gas phase boundary. In contrast, the diffraction spots of several other 2D liquids on graphite broaden with small increases in temperature.[36,37] The difference between O_2 and most other 2D and 3D liquids may be related to the O_2 liquid's extremely large stability range. (As mentioned in the Introduction, the ratio of critical to triple temperatures is about 2.5.) This large range indicates the liquid is more stable relative to the solid phase than in most other 2D systems. A lack of stability in the molecular-axis orientational order in the δ phase could cause the δ phase to be less stable relative to the liquid. Most current melting theories do not consider the stability of the liquid,[38] which is apparently important for O_2.

There are changes in the diffraction spots of the liquid and θ phase with increasing coverage at constant temperature. At the lowest coverages the radial width of the liquid diffraction spots is larger than at higher coverages. Measurements made at 39 K from a graphite crystal with first-order reflections having a radial width of about 0.06 Å^{-1} found about 0.16 Å^{-1} FWHM at low coverages and 0.10 Å^{-1} at higher coverages.[28] This would correspond

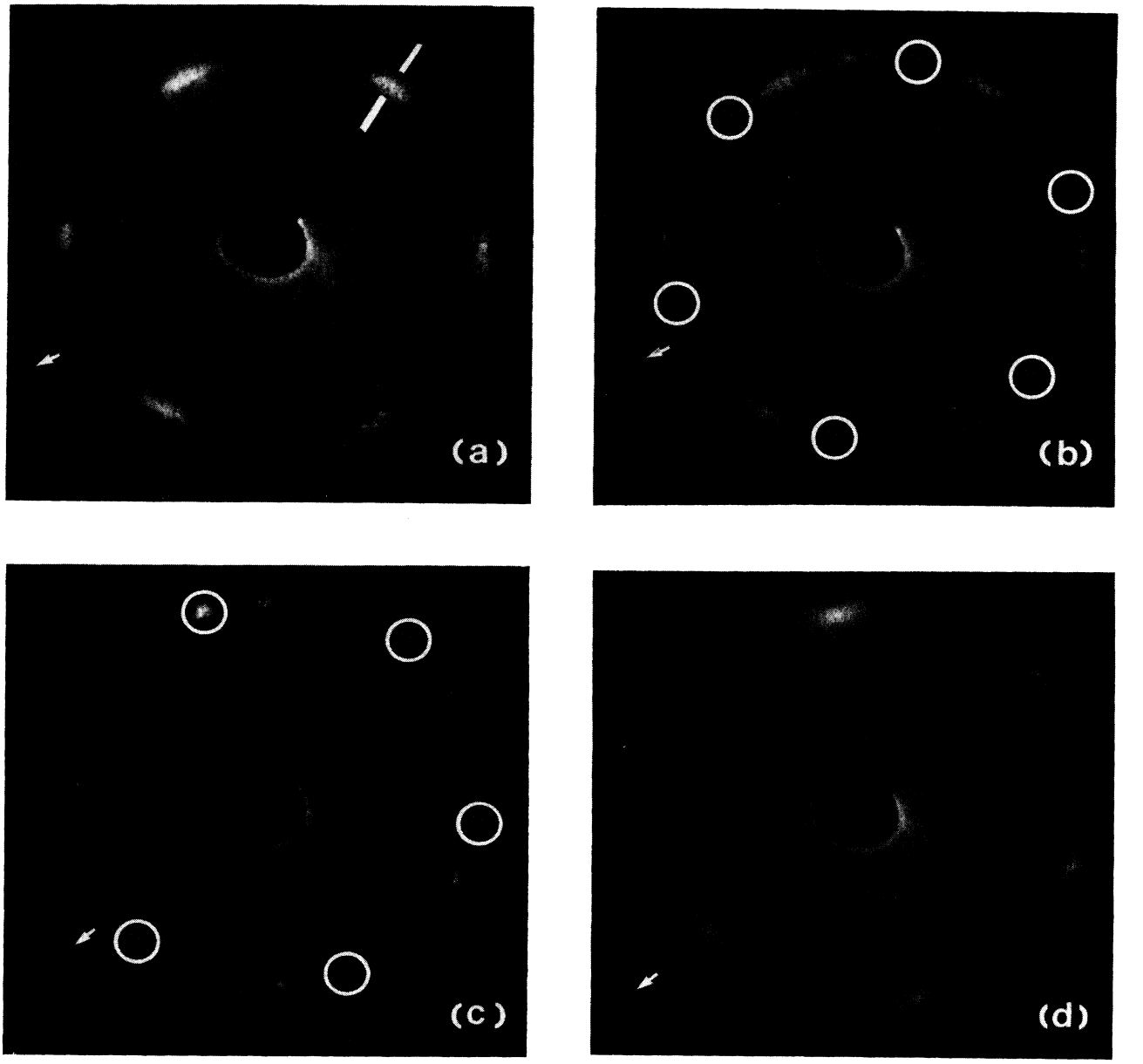

FIG. 5. LEED patterns from the higher-temperature phases. The arrows indicate the direction of a graphite first-order diffraction vector. (a) The liquid phase pattern at 39 K and 65 eV. (b) Coexistence between the liquid and θ phases at 39 K and 65 eV. Diffraction peaks from one domain of θ are circled. (c) The θ phase at 32 K and 65 eV. The diffraction peaks from one domain are circled and are slightly more intense than from the other domain. (d) The fluid phase at 32 K and 65 eV. Note epitaxial alignment along the arrow, 30° different from the liquid in (a). (See Ref. 33.)

to an increase with coverage in correlation length from about 10 Å to about 25 Å. The liquid's azimuthal width increases slightly with increasing coverage, and at coverages near the liquid-θ transition it is possible that the liquid diffraction spots actually consist of two broad, overlapping spots aligned a few degrees away from the direction of the graphite first-order diffraction vectors. There are no discernible changes in the θ phase spot widths with increasing coverage. However, as covering increases, the diffraction spots continuously rotate closer to the graphite (100) direction; the rotational epitaxy angle Ω defined in Fig. 6(b) increases from 20° to about 25.5° at the highest coverage measured. Because the diffraction spots in the θ and fluid may overlap in the transition region, we are not able to determine whether the θ to fluid phase transition is continuous or first order.

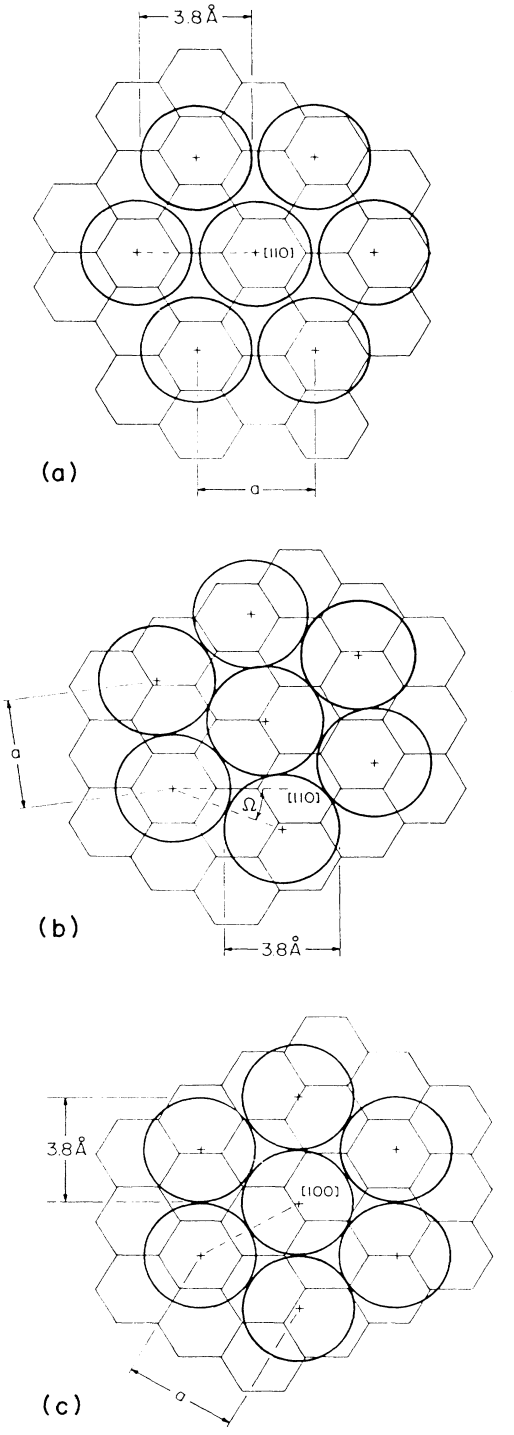

FIG. 6. Schematic representation of the local structure of the higher-temperature phases. All three structures are incommensurate; one molecule is arbitrarily shown in the center of a graphite hexagon. The molecular size shown is that of 3.8 Å for bulk liquid O_2 (Ref. 34). (a) The liquid phase is aligned along the graphite [110] direction with a typical nearest-neighbor spacing $a=4.0$ Å. (b) The θ phase is rotated $\pm 20°$ from the graphite [110] direction with a typical nearest-neighbor spacing $a=3.95$ Å. (c) The fluid phase is aligned along the graphite [100] direction with a typical nearest-neighbor spacing $a=3.85$ Å.

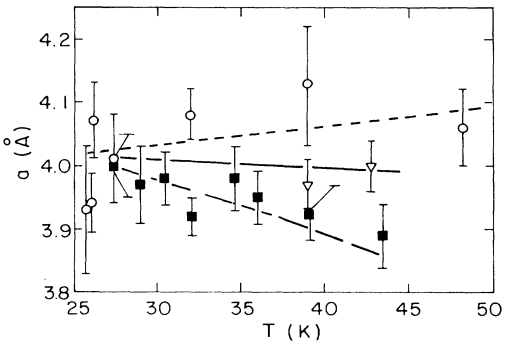

FIG. 7. Average nearest-neighbor distance a for the liquid and θ phases as a function of temperature. Liquid phase data are shown by the circles for low coverages close to the liquid-gas phase boundary and by the triangles for coverages just below the liquid-θ coexistence region. The lines are guides to the eye. The θ-phase data are shown by solid squares for coverages just above the liquid-θ coexistence region.

The lattice constant of the θ phase is close to that of Ar on graphite. However the rotational epitaxy angle of the θ phase (20°–26°) is substantially different from that of Ar on graphite (about 3°).[39] In addition, the rotational epitaxy of Ar on graphite changes by only 2° with a density increase of 5%,[39] while that of the θ phase changes by at least 6° with a density change of 4%. In the Novaco-McTague model[30,31] rotational epitaxy is determined by the overlayer to graphite mesh constant ratio and, to a lesser extent, by the overlayer longitudinal to transverse sound velocity ratio. The model correctly predicts the rotational epitaxy for Ar. The cause of the difference in rotational epitaxy between O_2 and Ar (and the Novaco-McTague model) could be due to the absence of internal degrees of freedom of the adsorbed species in the Novaco-McTague model; for example, there will be librational-vibrational coupling in the θ phase.

The diffraction spots in the liquid and fluid (see Fig. 5) are fairly sharp radially, so these phases have considerable short-range translational order ($\sim$20 and 15 Å correlation length, respectively).[28] Since these diffraction patterns do not consist of rings but have well-defined maxima and minima, the liquid and fluid phases[33] are well oriented with respect to the substrate. In other words, they have long-range bond-orientational order[36,38] which is probably imposed by the sixfold substrate field.

In the Novaco-McTague model the properties of solid overlayers that determine their rotational epitaxy are the phonon dispersion relations and the nearest-neighbor spacing.[30,31] Propagating collective modes with infinite lifetimes (phonons) do not exist in fluids, but fluids have propagating collective modes (both longitudinal and transverse) with finite lifetimes.[40] Thus, a model for the rotational epitaxy (direction of bond-orientational order) of fluid overlayers would include elements of the Novaco-McTague model[30,31] as well as the collective mode lifetimes. We are unaware of such a model.

The δ-liquid, δ-θ, δ^*-fluid, and δ'-fluid transitions are all first order, as evidenced by density changes, symmetry

changes, and two-phase coexistence over a temperature range of about 0.5 K. For submonolayer coverages (melting at the triple temperature) the δ-liquid coexistence range is 0.2 K. This nonzero range could be caused by a binding-energy heterogeneity[41,42] of only 0.1%. Above submonolayer coverages the coexistence range is 0.5 K, reflecting the intrinsic coexistence. For temperatures above about 31 K, the δ* phase melts into the fluid phase, but this is an apparently irreversible transition, since on cooling the fluid solidifies into the δ′ phase. The δ′ phase always melts into the fluid phase.

The δ-liquid and δ-fluid melting transitions were shown to be first order by the heat capacity and magnetic susceptibility data.[14–17] Analysis of heat capacity measurements to determine the entropy change at this transition produces values from $0.8k_B$ (from data in Ref. 15) to $1.3k_B$ (from data in Ref. 14), which is larger than the $0.4k_B$ value quoted for incommensurate Ne melting.[43] This larger entropy might be a result of the disordering of the O_2 molecular axes in the melting. For the δ-θ transition, Christoffer's data show two heat-capacity peaks, with the higher-temperature peak changing when a magnetic field is applied.[15] However, the relationship between the heat capacity data and the structural changes at the phase transition is not clear.

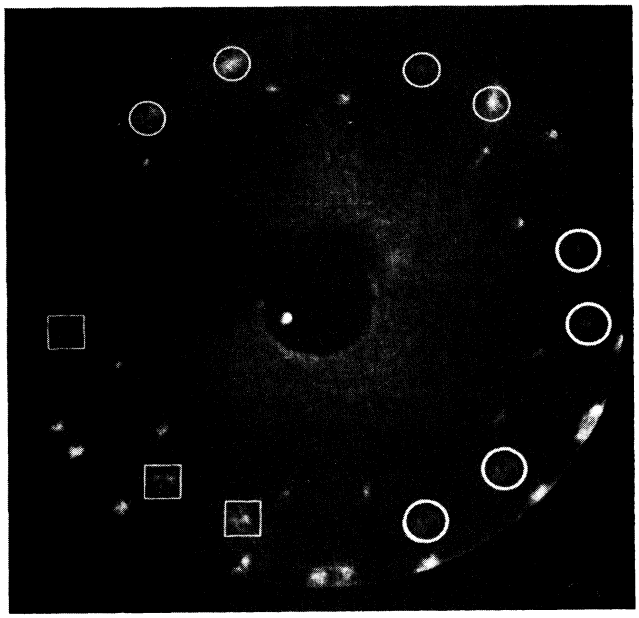

FIG. 8. LEED pattern from the θ phase at $T=28$ K and 65 eV showing the splitting into triplets. Inside the squares this splitting is resolved, while inside the circles it is not. The θ phase is coexisting with the δ phase, whose spots are not marked. The density of the θ phase in this picture is 0.075 ± 0.003 Å^{-2}. The lattice parameters as defined in Fig. 2 of Ref. 5 are $a_1=3.86\pm0.05$ Å, $a_2=3.99\pm0.08$ Å, $a_3=3.93\pm0.05$ Å, $\theta_1=60.2°\pm0.9°$, $\theta_2=58.2°\pm1.0°$, $\alpha_1=20.0°\pm1.0°$, $\alpha_2=20.2°\pm1.0°$, $\alpha_3=18.4°\pm0.5°$.

An examination of the θ phase diffraction pattern on the graphite crystals with smallest mosaic spread (such as crystal I of Ref. 5) reveals a splitting into triplets as shown in Fig. 8. This indicates the θ phase has a slightly oblique mesh similar to the ζ_1 phase.[5] Each spot in a triplet is resolution limited (as sharp as the δ phase spots) as expected for a 2D solid phase. Above about 30 K (not shown) no splitting could be resolved and the spots are not resolution limited. The width of the diffraction spots could be due to either an unresolved oblique solid structure or to a fluidlike nature for the θ phase at temperature above 30 K. Further measurements on high-quality single crystals will be needed to determine the nature of the θ phase above 30 K. Because of the absence of orientational ordering spots, we believe the θ phase has disordered molecular axis orientations.

V. SUMMARY

This study has examined some of the phases and phase transitions of O_2 adsorbed on single-crystal graphite; some of the results of this study and the earlier studies are summarized in the phase diagram shown in Figs. 1(b) and 9. Figure 9 is an expanded region of part of Fig. 1(b) from 10–50 K and 0.065–0.085 Å^{-2}. It summarizes the

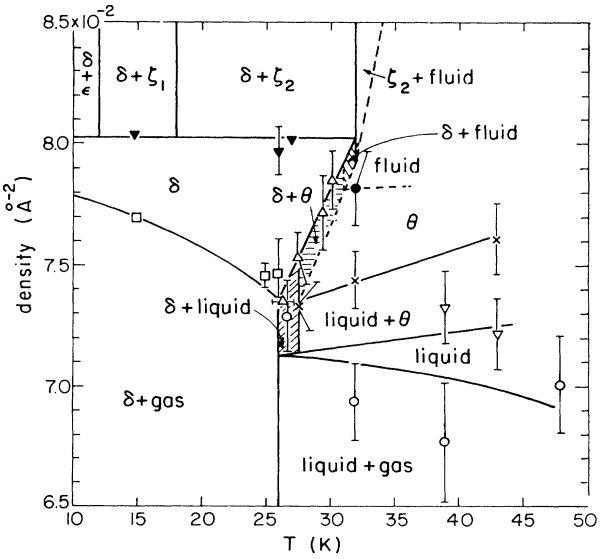

FIG. 9. Density-temperature phase diagram of O_2 adsorbed on graphite for 10–50 K and 0.065–0.085 Å^{-2}. The monolayer densities are deduced from diffraction measurements; possible adsorption in the second layer (if any) is not shown. The dashed lines are less certain phase boundaries than the solid lines. Open circles and open inverted triangles are the liquid phase densities at the liquid-gas and liquid-θ phase boundaries, respectively. The solid circle and the ×'s mark the θ phase boundaries. Open squares are the δ phase densities at the δ-gas phase boundary. Open triangles are the δ phase densities at the δ-θ ($T>27.5$ K) or δ-liquid ($26\text{ K}<T<27.5$ K) phase boundaries. Solid inverted triangles are the δ phase densities at the δ-ζ_2 ($T>18$ K) or δ-ζ_1 ($12\text{ K}<T<18$ K) phase boundaries. The δ′ phase was usually observed for densities near 0.080 Å^{-2}. The x-ray measurements from Refs. 9 and 10 are the points without error bars.

data presented in the earlier sections and earlier studies, shows the narrow two-phase coexistence regions not shown in Fig. 1(b), and shows the new triple lines at 27.5 and 31 K where, respectively, the δ, θ, and liquid and δ, θ, and fluid coexist. The phase boundaries were calculated from our data presented earlier (Figs. 4 and 7 and Fig. 3 of Ref. 5) and from diffraction data from other studies.[7-11]

We have measured the rotational epitaxy of the δ phase as a function of density and find there is a correlation between the rotational epitaxy and the skewing of the mesh (from a centered rectangle into an oblique mesh). We also observe a centered-rectangular δ^* phase at higher coverages, with an apparently first order δ-δ^* transition. Near the highest densities the δ' is also observed; this phase has a unit mesh that is the same as the high-density δ^* phase, but its rotational epitaxy is very different. Because we do not know the densities and temperatures where the δ' and δ^* phases are stable, they are not shown on the phase diagram.

The phase transitions of the δ phase into the higher-temperature liquid, θ, and fluid phases are all first order. Diffraction patterns from the liquid and fluid phases have been observed with LEED, and these phases have long-range bond-orientational order,[36,38] probably imposed by the substrate. We believe the θ phase is a solid with molecular axis disorder. Unexpectedly, the structural properties of the liquid, θ, and fluid phases do not change significantly between about 30 and 45 K. For the liquid (the only phase where additional data are available),[12,13] this could be related to an extremely large stability range. The rotational epitaxy of the θ phase and its change with density are very different from that of Ar on graphite,[39] even though the nearest-neighbor spacings are about the same.

The 2D phase diagram for O_2 on graphite is particularly rich and complicated. There are nine monolayer phases and six triple points known to date. The complexity and richness result from a competition between steric forces resulting from molecular shape, magnetic interactions, adsorbate-adsorbate forces, and lateral modulation of the adsorption energy caused by the substrate periodicity.

ACKNOWLEDGMENTS

We wish to thank O. E. Vilches for his constant interest in these experiments and for many useful discussions, and J. Suzanne, K. Flurchick, R. J. Birgeneau, S. Gregory, R. Marx, and their co-workers for communicating results prior to publication. We enjoyed useful and stimulating discussions with R. J. Birgeneau, M. Sutton, J. Suzanne, E. K. Riedel, M. Schick, R. D. Etters, L. Sorensen, and E. Wassermann. G. Felcher kindly provided us with an excellent supply of graphite crystals; Hoydoo You helped with a few of the experiments and provided many lively discussions; Jinhe Cui made width measurements of the spots. We acknowledge the support of the National Science Foundation Low Temperature Physics Program under Grant Nos. DMR 80-06334 and 85-13191 and one of us (M.F.T.) thanks the American Vacuum Society and the University of Washington for financial support.

*Present address: IBM Magnetic Recording Institute, IBM Almaden Research Center, San Jose, CA 95120-6099.

[1] *Ordering in Two Dimensions,* edited by S. K. Sinha (North-Holland, New York, 1980); J. G. Dash and J. Ruvalds, *Phase Transitions in Surface Films* (Plenum, New York, 1980); *Ordering in Strongly Fluctuating Condensed Matter Systems,* edited by T. Riste (Plenum, New York, 1980).

[2] O. E. Vilches, Ann. Rev. Phys. Chem. **31**, 463 (1980).

[3] M. F. Toney, R. D. Diehl, and S. C. Fain, Phys. Rev. B **27**, 6413 (1983).

[4] S. C. Fain, M. F. Toney, and R. D. Diehl, in *Proceedings of the Ninth International Vacuum Congress and Fifth International Conference on Solid Surfaces,* edited by J. L. de Segovia (Imprenta Moderna, Madrid, 1983), p. 129.

[5] M. F. Toney and S. C. Fain, Jr., Phys. Rev. B **30**, 1115 (1984).

[6] H. You and S. C. Fain, Jr., Phys. Rev. B **33**, 5886 (1986).

[7] J. P.. McTague and M. Nielsen, Phys. Rev. Lett. **37**, 596 (1976).

[8] M. Nielsen and J. P. McTague, Phys. Rev. B **19**, 3096 (1979).

[9] P. W. Stephens, P. A. Heiney, R. J. Birgeneau, P. M. Horn, J. Stoltenberg, and O. E. Vilches, Phys. Rev. Lett. **45**, 1959 (1980).

[10] P. A. Heiney, P. W. Stephens, S. G. J. Mochrie, J. Akimitsu, R. J. Birgeneau, and P. M. Horn, Surf. Sci. **125**, 539 (1983); P. A. Heiney, Ph.D. dissertation, Massachusetts Institute of Technology, 1982 (unpublished).

[11] S. G. J. Mochrie, M. Sutton, J. Akimitsu, R. J. Birgeneau, P. M. Horn, P. Dimon, and D. E. Moncton, Surf. Sci. **138**, 599 (1984).

[12] J. Dericbourg, Surf. Sci. **59**, 554 (1976).

[13] B. Gilquin, Docteur es Sciences these, Faculte des Sciences de l'Universite de Nancy, 1979 (unpublished).

[14] J. Stoltenberg and O. E. Vilches, Phys. Rev. B **22**, 2920 (1980).

[15] B. Christoffer, Diplom-Arbeit, University of Duisberg, 1983 (unpublished); R. Marx and B. Christoffer, J. Phys. C **18**, 2849 (1985); (unpublished).

[16] G. N. Lewis, Ph.D. dissertation, Cornell University, 1983 (unpublished); S. Gregory (private communication).

[17] U. Kobler and R. Marx, Phys. Rev. B (to be published).

[18] R. D. Etters, R. P. Pan, and V. Chandrasekharan, Phys. Rev. Lett. **45**, 645 (1980); R. P. Pan, R. D. Etters, K. Kobashi, and V. Chandrasekharan, J. Chem. Phys. **77**, 1035 (1982).

[19] R. D. Etters and O. M. B. DuParc, Phys. Rev. B **32**, 7600 (1985); O. M. B. DuParc and R. D. Etters, J. Chem. Phys. **86**, 1020 (1987).

[20] K. Flurchik and R. D. Etters, J. Chem. Phys. **84**, 4657 (1986).

[21] S. Tang, S. D. Mahanti, and R. K. Kalia, Phys. Rev. Lett. **56**, 484 (1986).

[22] Y. P. Joshi and D. J. Tildesley, Surf. Sci. **166**, 169 (1986).

[23] V. R. Bhethanabotla and W. A. Steele (unpublished).

[24] O. E. Vilches (private communication).

[25] X-ray measurements on single-crystal graphite have found that

hours can be required for phase transitions to occur for xenon near 50 K. R. J. Birgeneau (private communication).
[26]R. D. Diehl and S. C. Fain, Jr., Surf. Sci. **125**, 116 (1983).
[27]M. F. Toney, Ph.D. dissertation, University of Washington, 1983 (unpublished).
[28]The spot widths reported in Ref. 27 have systematic errors. The widths reported here were measured by Jinhe Cui using a calibrated microdensitometer.
[29]R. F. W. Bader, W. H. Henneker, and P. E. Cade, J. Chem. Phys. **46**, 3341 (1967).
[30]J. P. McTague and A. D. Novaco, Phys. Rev. B **19**, 5299 (1979).
[31]A. D. Novaco and J. P. McTague, Phys. Rev. Lett. **38**, 1286 (1977).
[32]L. W. Bruch, Surf. Sci. **115**, L67 (1982).
[33]Heat capacity measurements (Ref. 14) show that the low-density higher-temperature phase clearly has more disorder than the δ phase. Because this phase coexists with a very-low-density gas phase, it is called a liquid. The higher-density poorly ordered phase which we call a fluid has a different orientational epitaxy with respect to the graphite and does not coexist with a gas.
[34]H. W. Furumoto and C. H. Shaw, Phys. Fluids **7**, 1026 (1964); D. G. Henshaw, Phys. Rev. **119**, 22 (1960); K. S. Pedersen, F. Y. Hansen, and K. Carneiro, J. Chem. Phys. **70**, 1051 (1979).
[35]Average spacings for the poorly ordered phases were calculated by assuming a sixfold triangular nearest-neighbor coordination. The error associated with this method is probably less than the uncertainty in the experimental data.
[36]S. E. Nagler, P. M. Horn, T. F. Rosenbaum, R. J. Birgeneau, M. Sutton, S. G. J. Mochrie, D. E. Moncton, and R. Clarke, Phys. Rev. B **32**, 7373 (1985).
[37]J. M. Gay, J. Suzanne, and R. Wang, J. Phys. (Paris) **46**, L425 (1985).
[38]D. R. Nelson and B. I. Halperin, Phys. Rev. B **19**, 2457 (1979); S. Ostlund and B. I. Halperin, *ibid.* **23**, 335 (1981).
[39]C. G. Shaw, S. C. Fain, Jr., and M. D. Chinn, Phys. Rev. Lett. **41**, 955 (1978).
[40]J. P. Hansen and I. R. McDonald, *Theory of Simple Liquids* (Academic, New York, 1976).
[41]J. G. Dash and R. D. Puff, Phys. Rev. B **24**, 295 (1981).
[42]R. E. Ecke, J. G. Dash, and R. D. Puff, Phys. Rev. B **26**, 1288 (1982).
[43]G. B. Huff and J. G. Dash, J. Low. Temp. Phys. **24**, 155 (1976).

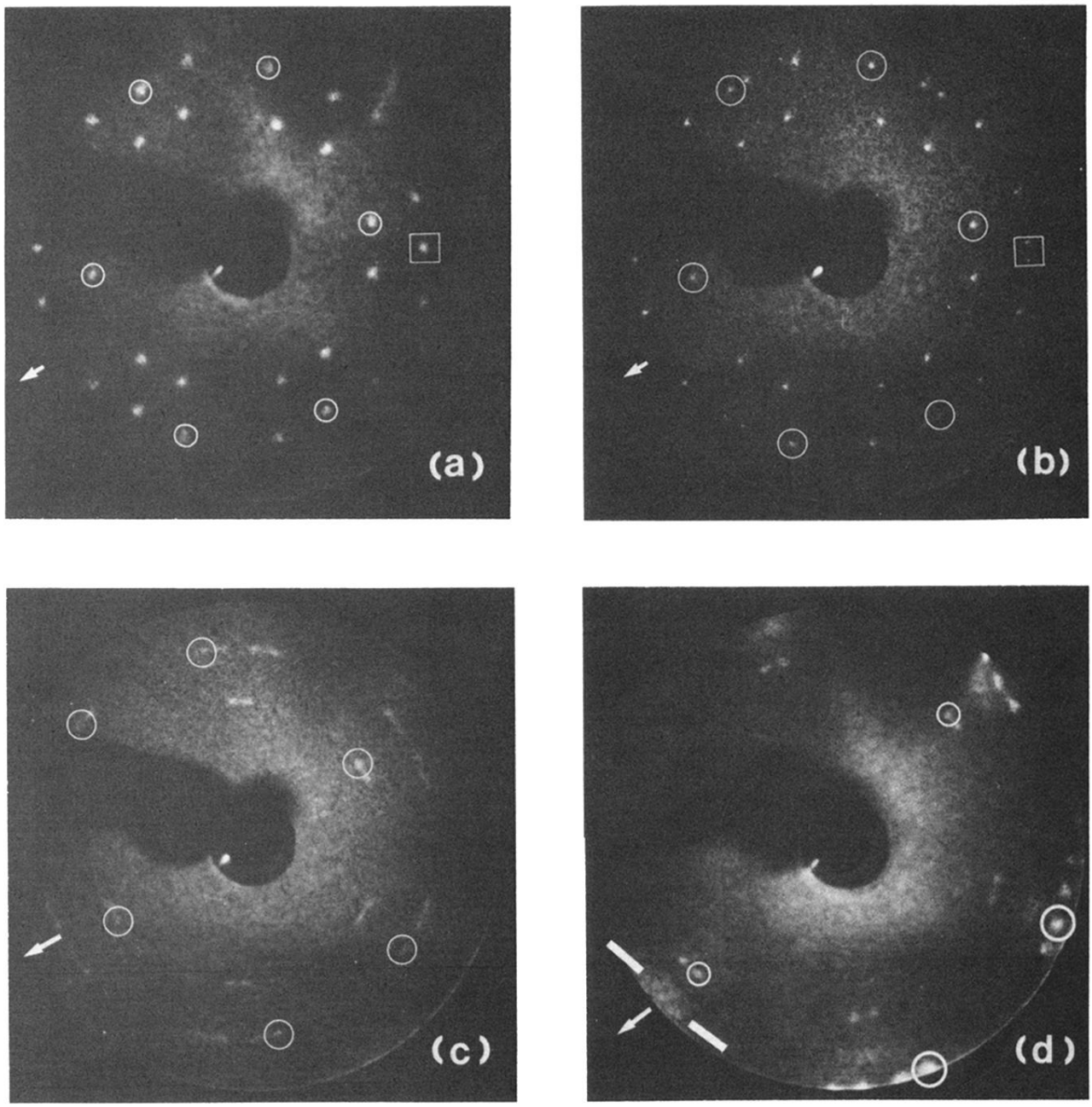

FIG. 2. LEED patterns from the δ phase. The diffraction from one domain is indicated by the circles. The squares indicate one set of spots that is split in (b), but almost degenerate in (a). The arrows indicate the direction of a graphite first-order diffraction vector. There is some distortion caused by the LEED apparatus in the upper right corners of (a) and (d). (a) The low-coverage δ phase at an electron energy of 110 eV, a temperature of 23 K, and a density of 0.075 Å^{-2}. (b) The high-coverage δ* phase at 110 eV, 21 K, and 0.077 Å^{-2}. (c) The δ′ phase at 112 eV, 16 K, and a density of 0.080 Å^{-2}. The azimuthal smearing of the spots is discussed in Ref. 3. (d) The δ′ phase at 65 eV, 31.8 K, and a density at which the δ′ phase coexists with the fluid phase discussed in Sec. IV. One diffraction spot from the fluid phase is located between the two white lines. The different graphite orientation is due to a different graphite substrate than (a)–(c).

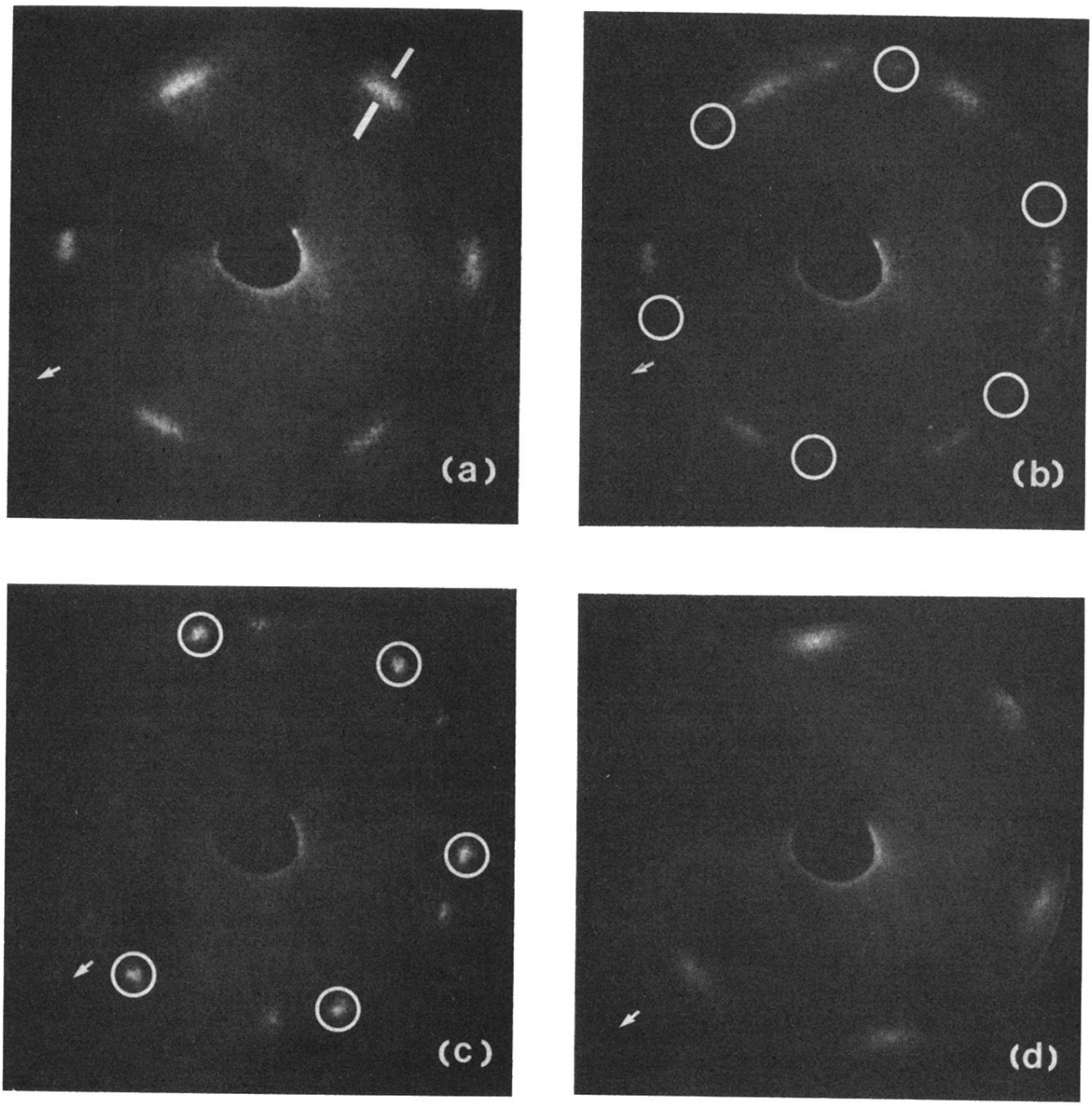

FIG. 5. LEED patterns from the higher-temperature phases. The arrows indicate the direction of a graphite first-order diffraction vector. (a) The liquid phase pattern at 39 K and 65 eV. (b) Coexistence between the liquid and θ phases at 39 K and 65 eV. Diffraction peaks from one domain of θ are circled. (c) The θ phase at 32 K and 65 eV. The diffraction peaks from one domain are circled and are slightly more intense than from the other domain. (d) The fluid phase at 32 K and 65 eV. Note epitaxial alignment along the arrow, 30° different from the liquid in (a). (See Ref. 33.)

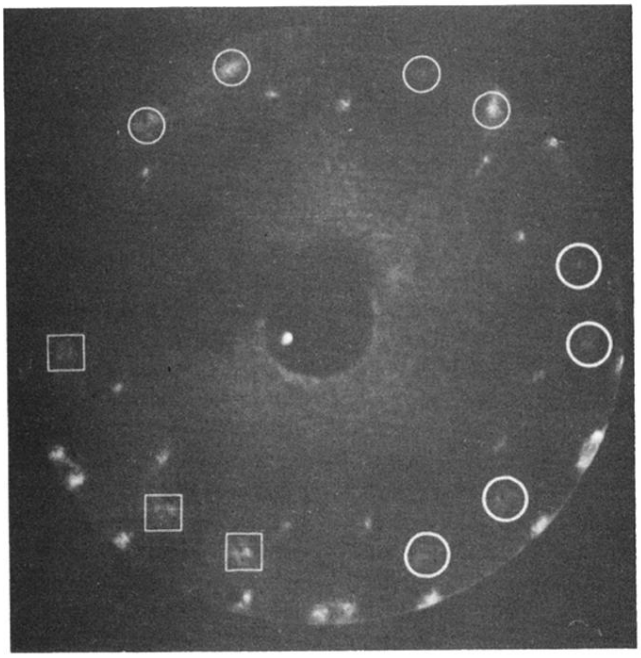

FIG. 8. LEED pattern from the θ phase at $T=28$ K and 65 eV showing the splitting into triplets. Inside the squares this splitting is resolved, while inside the circles it is not. The θ phase is coexisting with the δ phase, whose spots are not marked. The density of the θ phase in this picture is 0.075 ± 0.003 Å^{-2}. The lattice parameters as defined in Fig. 2 of Ref. 5 are $a_1=3.86\pm0.05$ Å, $a_2=3.99\pm0.08$ Å, $a_3=3.93\pm0.05$ Å, $\theta_1=60.2°\pm0.9°$, $\theta_2=58.2°\pm1.0°$, $\alpha_1=20.0°\pm1.0°$, $\alpha_2=20.2°\pm1.0°$, $\alpha_3=18.4°\pm0.5°$.